(Received 25 October 2024, Accepted 12 December 2024, Scheduled 19 December 2024)

# Tumor Detection and Imaging through Body Scanning Using TMSA Operating in MBAN Band

Satheesh Rao*

*Department of Electronics and Communication Engineering, NMAM Institute of Technology, Nitte (Deemed to be University), India*

**ABSTRACT:** In this article, body scanning and imaging using a triangular microstrip antenna (MSA) with microstrip line feeding is presented. The resonant frequency of this antenna is 2.383 GHz having 20 dB bandwidth 3 MHz. The results comply with the 2.36 to 2.39 GHz band that the Federal Communication Commission (FCC) has designated for medical related applications. This antenna is used in scanning the human body model to detect the presence of tumor. The scan results are used to generate a 2-D color contour plot, which shows the location of tumor. Parametric analysis is carried out to fix the slot dimension to get optimum antenna performance. After successful simulation, the antenna structure is fabricated, and testing is carried out using Power Network Analyzer.

## 1. INTRODUCTION

These days, diagnosing patients with acute diseases requires the use of costly body scanning technology like X-rays, CT scans, and magnetic resonance imaging (MRI). These tools can identify a wide range of medical conditions, including tumors, malignant cells, fractures, etc. Patients are susceptible to ionising radiation when being scanned with such devices. Additionally, patients must pay a large sum of money for scanning due to the high cost of scanning. Breast cancer is one of the top causes of death worldwide. Breast cancer cells usually form tumor. Early detection of such tumors can totally cure breast cancer, lowering the overall fatality rate from the disease. Microstrip antenna (MSA) based imaging can be a useful way to undertake breast cancer screening tests at a low cost.

Wireless communication efficiently uses an antenna as a sensing device [7–16]. Once the antenna is tuned to the suitable medical body area network (MBAN) band, patients' bodies can also be scanned with it. Various types of patch antennas have been documented in the literature for the detection of foreign bodies, tumours, and breast cancer [13–15]. Several ultra-wideband antennas have been reported for biomedical use, including E-shaped, crescent shaped, and other designs [13–17]. The aforementioned reported works lack theoretical analysis, have complex geometry, or have frequency bands that are outside the FCC's recommended spectrum for body area networks [19, 20, 25, 26].

In this article, a triangular microstrip antenna is proposed for the detection of tumor. The antenna resonates at 2.363 GHz with 3 MHz bandwidth useful for biomedical applications. Further using this antenna detection of tumor and imaging is carried out via body scanning.

## 2. ANTENNA GEOMETRY

The microstrip line fed patch antenna is shown in Fig. 1. The antenna has a radiating dimension of $L \times W \times h\,\text{cm}^3$ on which the radiating patch has an equilateral triangle shape with side $S_a$ cm. The dimension of feed line that uses inset cut for matching is $(L_m \times W_m)\,\text{cm}^2$, and the inset with a dimension of $L_i \times W_i)\,\text{cm}^2$ is excited via a 50 Ω SMA connector. The antenna is designed on an Arlon AD1000 substrate that is 0.635 mm thick with microstrip line feeding. Table 1 shows the dimensions of designed antenna in cm. Fig. 2 show the fabricated antenna on an Arlon AD1000 substrate. Since the antenna under consideration is of narrow band, a substrate with higher dielectric constant is desirable. Hence, an Arlon AD1000 substrate is chosen that has dielectric constant of 10.2, and it is suitable for narrow band applications.

**TABLE 1.** Dimensions of the designed antenna [27].

| Variable | Dimension (in cm) |
|---|---|
| $L$ | 5.2506 |
| $W$ | 5.2506 |
| $S_a$ | 2.635 |
| $L_m$ | 1.242 |
| $W_m$ | 0.1 |
| $L_i$ | 0.4 |
| $W_i$ | 0.33 |
| $h$ | 0.0635 |

The resonant frequency of triangular antenna is as in Equation (1) [1–4]

$$f_{m,n} = \frac{2c}{3S_a\sqrt{\epsilon_{re}}}\sqrt{m^2 + mn + n^2} \tag{1}$$

* Corresponding author: Satheesh Rao (satheesh.rao@nitte.edu.in).

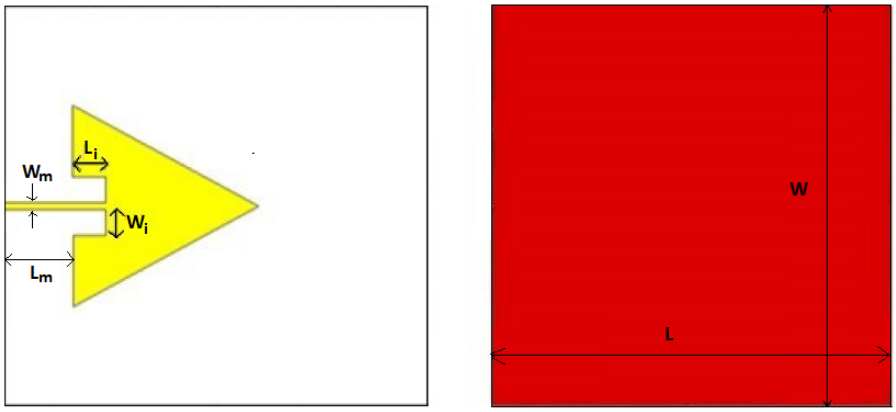


**FIGURE 1**. Proposed antenna for tumor detection applications top and bottom view.

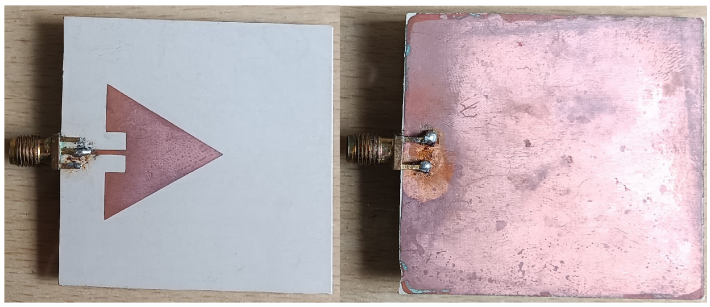

**FIGURE 2**. Fabricated antenna top and bottom views.

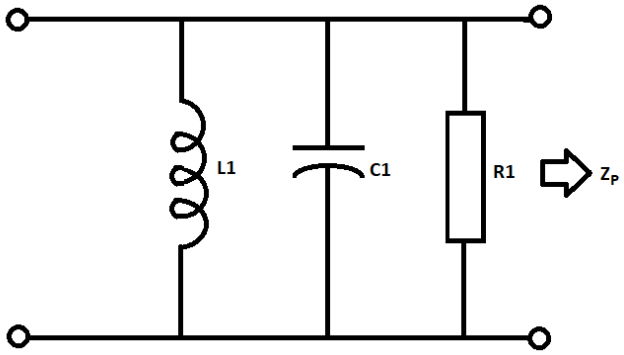


**FIGURE 3**. Equivalent network for rectangular patch.

For $TM_{10}$ mode, $S_a$ is changed to $S_{ae}$ for more precision. Hence, Equation (2) provides the resonance frequency.

$$f_{1,0} = \frac{2c}{3S_{ae}\sqrt{\epsilon_{re}}} \tag{2}$$

The effective side length of the triangular patch is given by Equation (3)

$$S_{ae} = S_a\left[1 + 2.199\frac{h}{S_a} - 12.853\frac{h}{S_a\sqrt{\epsilon_{re}}}16.436\frac{h}{S_a\epsilon_{re}} + 6.182\left(\frac{h}{S_a}\right)^2 - 9.802\left(\frac{h}{S_a}\right)^2\frac{1}{\sqrt{\epsilon_{re}}}\right] \tag{3}$$

### 2.1. Theoretical Analysis

The active radiating structure of triangular MSA (TSMA) can be modelled by radio frequency (RF) equivalent R-L-C circuit using rectangular patch area equivalence method. The network is as shown in Fig. 3. The values of inductance, capacitance, and resistance can be computed using Equations (4)–(6) [5, 6, 22, 23].

$$C_1 = \frac{LW\varepsilon_0\varepsilon_e}{2h}\cos^{-2}\left(\frac{\pi X_0}{L}\right) \tag{4}$$

$$R_1 = \frac{Q}{\omega_r^2 C_1} \tag{5}$$

$$L_1 = \frac{1}{\omega_r^2 C_1} \tag{6}$$

$$Q = \frac{c\sqrt{\varepsilon_{re}}}{hf_r} \tag{7}$$

$\varepsilon_{re}$ — effective dielectric constant.

The feeding line can be represented as inductance L, capacitance C and is shown in Fig. 4 [23, 24]

$$L_n = 0.4h\left(\sqrt{\frac{W_s}{H}} - 1.0525\right)\ \mu\text{H} \tag{8}$$

$$C_n = W_s(0.0095\varepsilon_r + 0.00125)W_s/h + 0.0052\varepsilon_r + 0.007\}\ \text{nF} \tag{9}$$

where

$$\varepsilon_{re} = 1/2[(\varepsilon_r + 1) + (\varepsilon_r - 1)(1 - 12h/W_s)^{-1/2} \tag{10}$$

The final radio frequency equivalent network for the proposed antenna is as depicted in Fig. 5. Its overall impedance $Z_{in}$ can be computed from Equation (11). The resonant frequency of this circuit is as in Equation (12)

$$Z_{in} = Z_p||Z_m \tag{11}$$

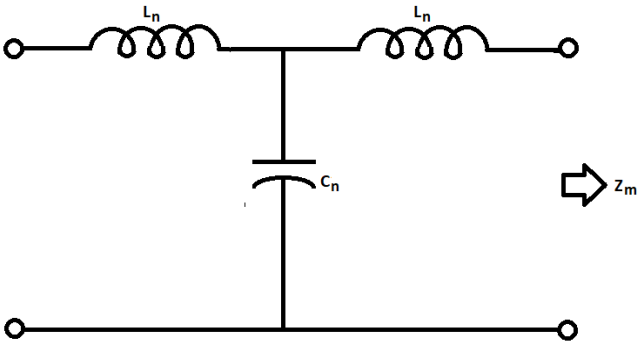


**FIGURE 4**. RF equivalent circuit for stripline.

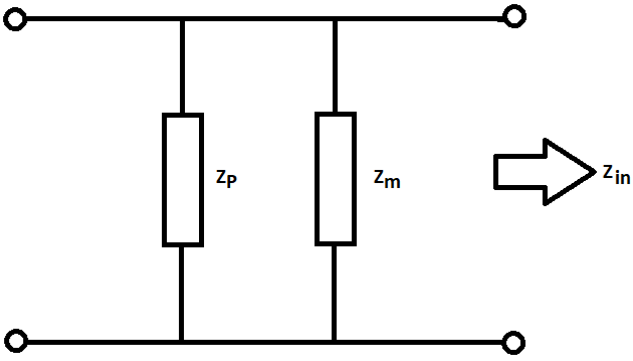


**FIGURE 5**. Radio frequency equivalent for the antenna.

$$f_C = \frac{1}{2\pi\sqrt{LC}} \tag{12}$$

### 2.2. Tumor Detection Methodology

The electrical characteristics of various human tissues or organs vary, including conductivity, mass, and dielectric constant. The capacitance offered by the body, i.e., Cbody and resistance, i.e., Rbody, can be used to simulate the human body. The equivalent impedance of the antenna and the body network is parallel when the antenna is placed over the human body. The resonant frequency of this network will be determined by its effective impedance. The resonant frequency falls as the overall impedance rises. The electrical characteristics of tumours differ from those of normal tissues. Tumours have a greater conductivity and dielectric constant; hence, the effective body impedance will be larger than normal tissue. Therefore, the presence of a tumor in the body will lead to a greater fall of resonant frequency, which shows the tumor existence. The designed antenna is mounted over a human body model. Fig. 6 shows the equivalent circuit. The body capacitance is dielectric dependent. Tumor cells have different dielectric constants from the healthy cells. Whenever there exists a tumor at a particular location on human body, the capacitance offered by the body at that location changes, leading to change in the resonant frequency of the antenna.

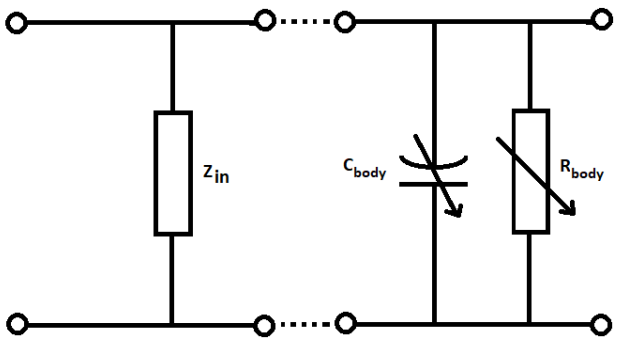


**FIGURE 6**. Equivalent network for antenna placement on body.

## 3. RESULTS AND DISCUSSION

### 3.1. Simulation

The TMSA is simulated, and the simulated result is shown in Fig. 7. Inset fed TMSA resonates at 2.383 GHz with $S_{11}$ of $-31.618$ dB. Since body capacitance acts as capacitive loading to this antenna that has narrow bandwidth, any change in body capacitance will be more accurately sensed by this structure. The designed TMSA operates in the FCC's Medical Body Area Network band. Computer Simulation Technology (CST) Microwave Studio suite 18 is used in this design.

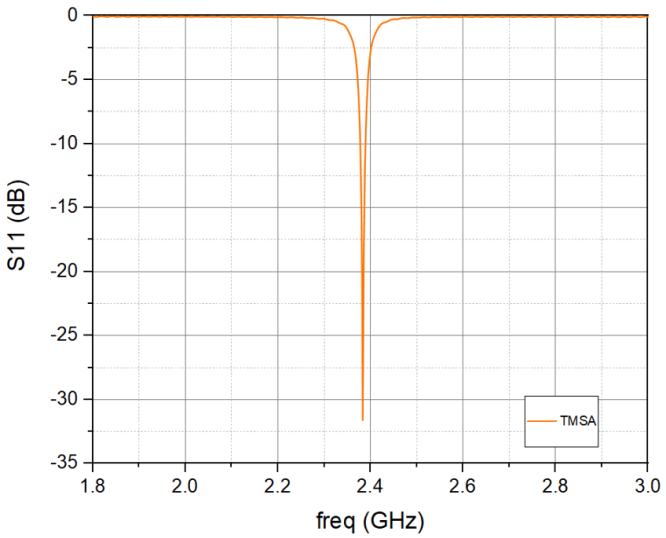


**FIGURE 7**. Plot of $S_{11}$ — Simulated for TMSA.

### 3.2. Fabrication and Testing

The triangular MSA is fabricated on an Arlon AD1000 substrate. The dielectric constant of the substrate is 10.2. Fig. 8 shows fabricated antenna's top view and bottom view. The $S_{11}$ of the fabricated antenna is obtained using Agilent Power Network Analyzer (PNA), and the outcomes are depicted in Fig. 9. Greater match is seen in the test result with the simulation one, with minimum deviation due to the unequal procedure of manufacturing. Fabricated TMSA resonates at 2.39 GHz with reflection coefficient $-19.01$ dB.

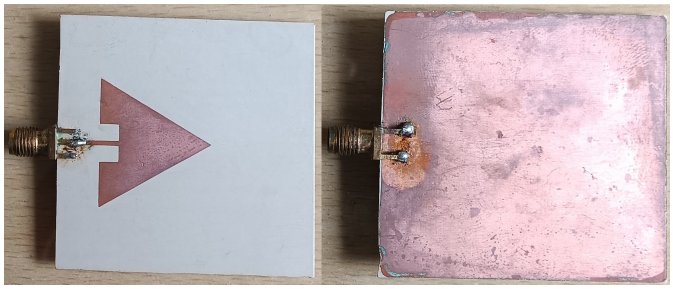

**FIGURE 8**. Fabricated antenna top and bottom views.

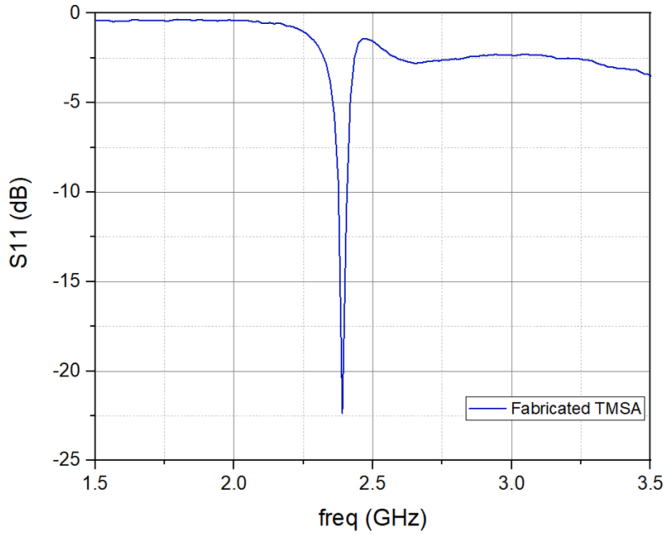


**FIGURE 9**. Plot of $S_{11}$ — For fabricated TMSA.

### 3.3. Body Phantom on CST Studio

Using CST studio, body mimicking phantom is designed, and a TMSA is mounted on this model. The simulation setup is as depicted in Fig. 10. Simulation is carried out considering body model and body model with tumor. The simulation outcomes are as in Fig. 11. Both the resonant frequency and reflection coefficient's amplitude change are noted. The body model with tumor has a stronger wave reflection, with a reflection coefficient $S_{11}$ of $-16.46$ dB, whereas the body model without tumor has a reflection coefficient value of $-17.82$ dB. A shift in the resonance frequency also exists. The tumor's higher dielectric constant causes a rise in effective body capacitance, which lowers the resonant frequency. The antenna resonating at 2.346 GHz for the body model without a tumor tends to resonate at 2.34 GHz for the body model with a tumor cell. The resonance frequency is 6 MHz lower with a tumor than it would be without one. To examine the effect of tumor size on the performance of the system, simulation is repeated by varying the size of the tumor [18, 21]. The tumor size is varied from 2 mm to 8 mm, and its effect on reflection coefficient is noted. It is observed from the simulation that, as tumor size increases, the reflection coefficient increases. This increase in the reflection coefficient is due to the increase in the amount of signal reflected from the tumor as size increases. The results are as shown in Fig. 12. This data can be utilized in identifying the tumor size.

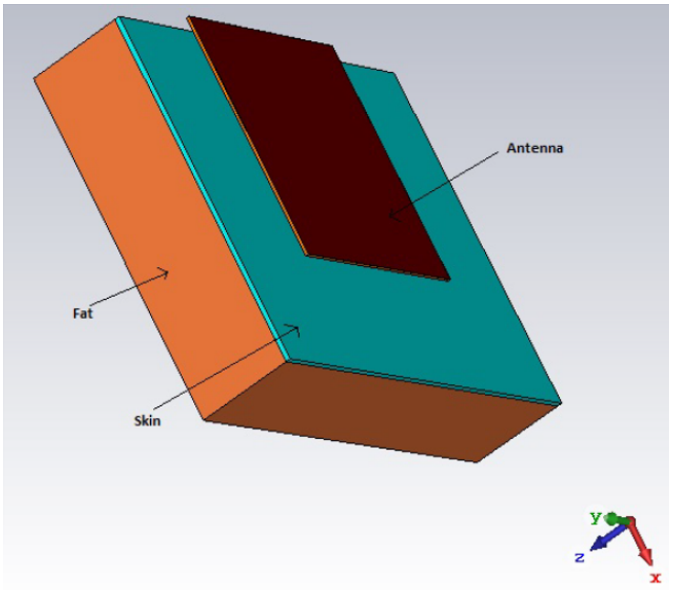


**FIGURE 10**. Antenna placement on body model.

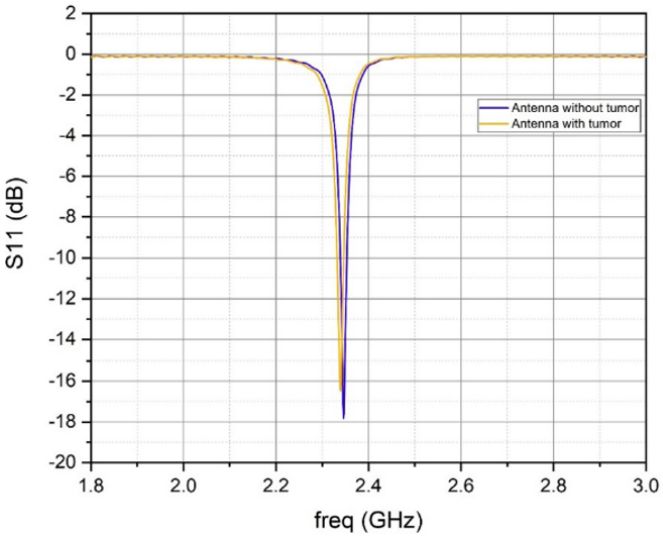


**FIGURE 11**. Plot of $S_{11}$ — For body model simulation with and without tumor.

### 3.4. Body Phantom for Testing

The experimental setup created [27] to evaluate the constructed TMSA on the body model is seen in Fig. 13. Petroleum jelly is used to build the body model's fat layer, and a combination of water and wheat flour is used to imitate the tumor. Table 2 lists these materials' electrical characteristics. The body model with and without a tumour is used to assess the reflection coefficients when the constructed TMSA is put on this model. In Fig. 14, the test results are displayed. It is observed that the $S_{11}$ rises to $-12.7$ dB with a body model while remaining at $-19.01$ dB without one. Additionally, the resonant frequency shifts to 2.38 GHz from 2.39 GHz. This is because the body model introduces a change in the dielectric characteristic. The resonance frequency shifts to 2.3 GHz, and the reflection coefficient increases to $-8.36$ dB when the antenna $S_{11}$ evaluated

**TABLE 2**. Material's electrical properties [27].

| Parts | Material used | Dielectric Constant | Conductivity S/m |
|---|---|---|---|
| **Fat** | *Petroleum Jelly* | 2.36 | 0.012 |
| **Tumor** | *Wheat Flour and water mix* | 28.1 | 1.32 |

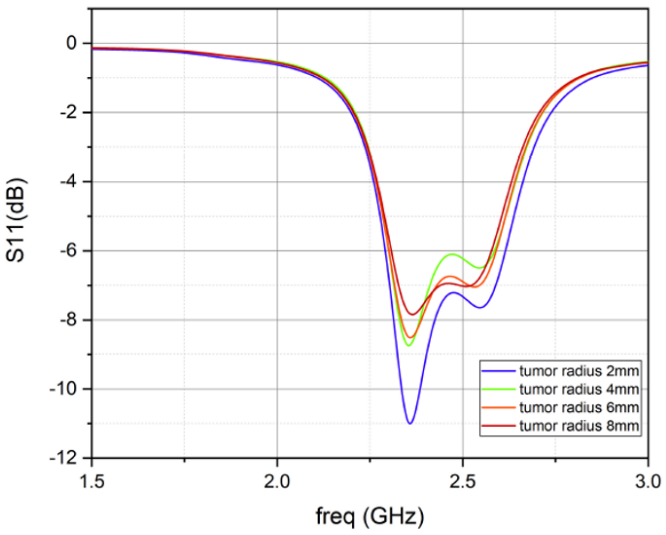


**FIGURE 12**. Plot of $S_{11}$ — For body model simulation with tumor of varying size.

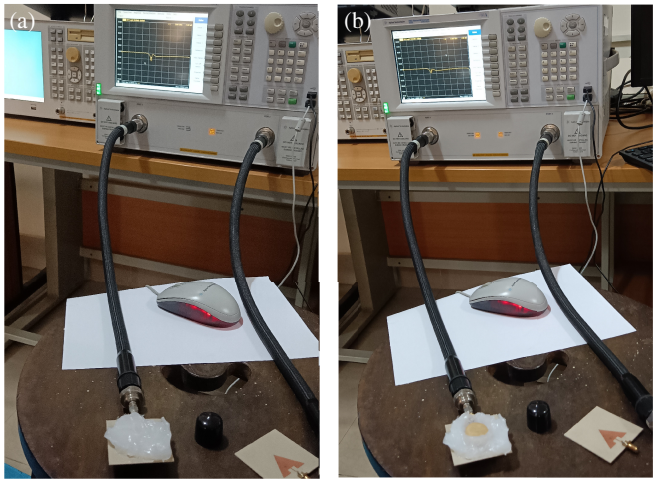


**FIGURE 13**. Experimental setup for TMSA, (a) non-tumor and (b) tumor.

by adding the tumor to the model. When a tumor is present, there is a 0.8 GHz change in the resonance frequency.

### 3.5. Body Scanning and 2D-Imaging

Inset fed TMSA is placed 2 mm above the body model created in CST tool. The antenna is made to move in both $x$ and $y$ directions, and simulation is carried out for every 5 mm movement of the antenna. Fig. 15 shows the position of the radiating

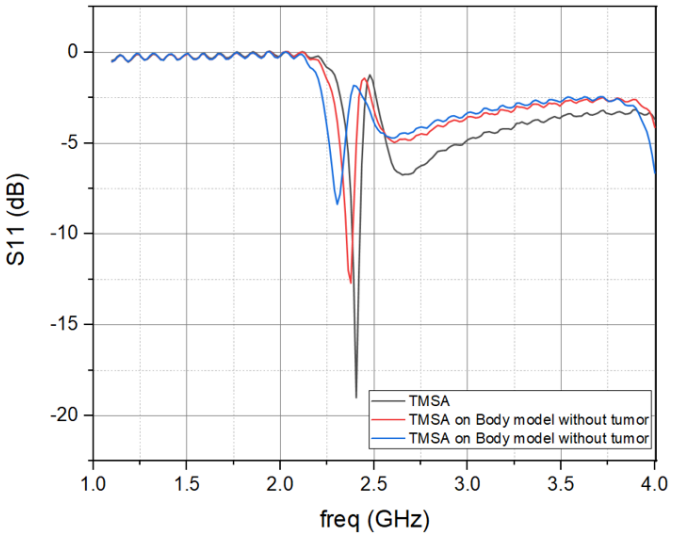


**FIGURE 14**. Plot of $S_{11}$ — Measured result for TMSA mounted on body model.

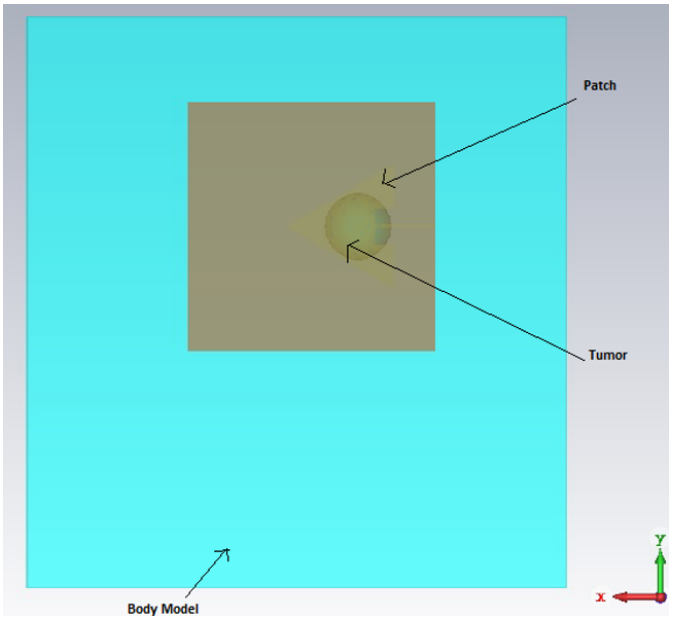


**FIGURE 15**. Radiating patch falling above the tumor.

patch of triangular antenna falling just above the tumor for $x$ axis position $-5$ mm and $y$ axis position $-5$ mm w.r.t the global co-ordinate system. The scanning process covered an area of $70 \times 50\,\text{mm}^2$ covering the tumor and its surrounding. The size of the tumor inserted into the body model is of 7 mm radius. Position of the antenna for $x = -30$ mm and $y = -5$ mm is

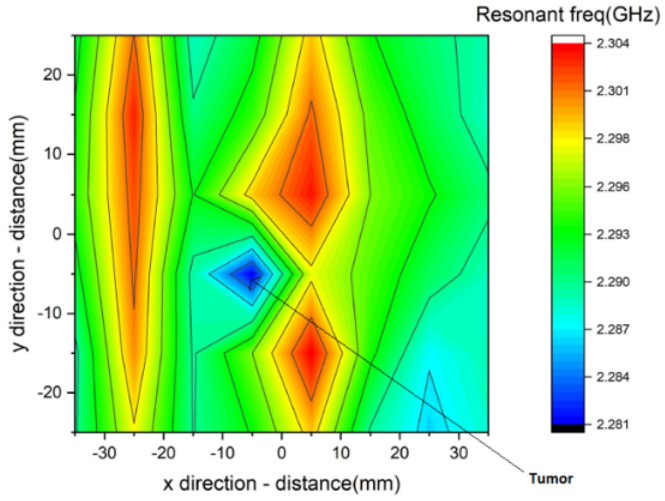


**FIGURE 16**. 2-D color contour plot.

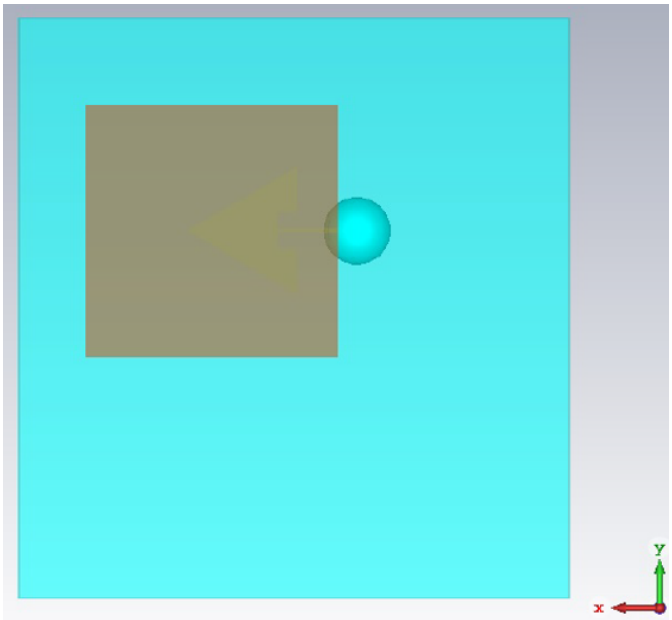


**FIGURE 17**. Antenna position for $x = -30$ mm and $y = -5$ m.

as shown in Fig. 17, and Fig. 18 shows the antenna position for $x = 10$ mm and $y = -5$ mm.

For every $x$ and $y$ position scan, the resonant frequency is noted down from $S_{11}$ plot. These values along with $x$ and $y$ locations are used to create a two-dimensional matrix. This 2-D array of data points is used to plot a color contour image. The resultant 2-D image is as shown in Fig. 16. In this image, variation in the resonant frequency is mapped to varying color where $x$ and $y$ axes represent the antenna position. The presence of tumor is clearly visible in Fig. 16 which is shown as blue color patch. We can see a single blue patch for antenna position $x = -5$ mm and $y = -5$ mm that was the location where tumor was inserted into the body model.

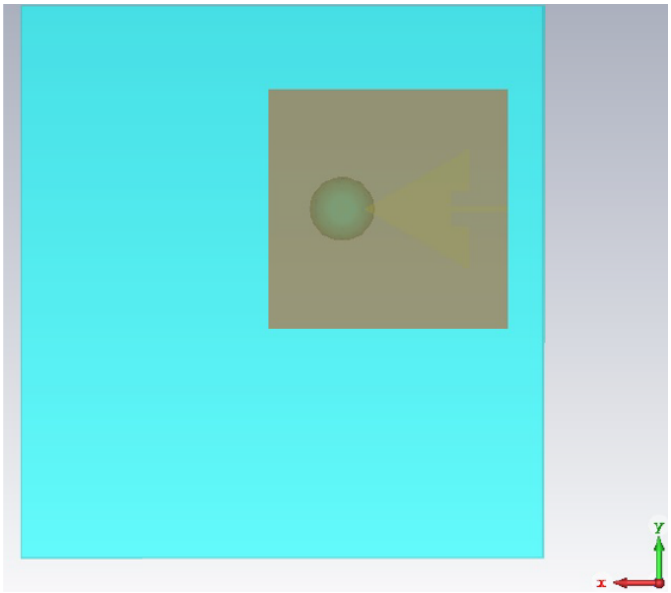


**FIGURE 18**. Antenna position for $x = 10$ mm and $y = -5$ mm.

## 4. CONCLUSION

A microstrip line fed triangular MSA for biomedical application has been designed, experimented, and presented. The designed antenna meets the specifications set by FCC for MBAN band. The findings of the simulation show that the antenna can detect tumours with great clarity. Further through simulation, the designed antenna is used to scan the human body model, and the result is used to create a 2-D color map that clearly shows the presence of tumor and its location.

## REFERENCES

[1] Singh, A., K. Shet, D. Prasad, A. K. Pandey, and M. Aneesh, "A review: Circuit theory of microstrip antennas for dual-, multi-, and ultra-widebands," in *Modulation in Electronics and Telecommunications*, 105–123, G. Dekoulis (ed.), IntechOpen, 2020.

[2] Singh, A., M. Aneesh, Kamakshi, and J. A. Ansari, "Analysis of microstrip line fed patch antenna for wireless communications," *Open Engineering*, Vol. 7, No. 1, 279–286, 2017.

[3] Minasian, A. A. and T. S. Bird, "Particle swarm optimization of microstrip antennas for wireless communication systems," *IEEE Transactions on Antennas and Propagation*, Vol. 61, No. 12, 6214–6217, 2013.

[4] Deeksha, B., A. S. R. Teja, E. S. Laxshmi, M. N. Eshwar, A. Singh, and M. Aneesh, "Electromagnetically coupled notches loaded patch antenna for bio-medical applications," in *2017 International Conference on Multimedia, Signal Processing and Communication Technologies (IMPACT)*, 283–286, Aligarh, India, Nov. 2017.

[5] Bahl, I. J., *Lumped Elements for RF and Microwave Circuits*, Artech House, 2022.

[6] Balanis, C. A., *Antenna Theory: Analysis and Design*, John Wiley & Sons, 2015.

[7] See, C. H., R. A. Abd-Alhameed, D. Zhou, T. H. Lee, and P. S. Excell, "A crescent-shaped multiband planar monopole antenna for mobile wireless applications," *IEEE Antennas and Wireless*

*Propagation Letters*, Vol. 9, 152–155, 2010.

[8] Kissi, C., M. Särestöniemi, T. Kumpuniemi, S. Myllymäki, M. Sonkki, M. N. Srifi, H. Jantunen, and C. Pomalaza-Raez, "Reflector-backed antenna for UWB medical applications with on-body investigations," *International Journal of Antennas and Propagation*, Vol. 2019, No. 1, 6159176, 2019.

[9] Yang, F., X.-X. Zhang, X. Ye, and Y. Rahmat-Samii, "Wide-band E-shaped patch antennas for wireless communications," *IEEE Transactions on Antennas and Propagation*, Vol. 49, No. 7, 1094–1100, 2001.

[10] Conway, G. A. and W. G. Scanlon, "Antennas for over-body-surface communication at 2.45 GHz," *IEEE Transactions on Antennas and Propagation*, Vol. 57, No. 4, 844–855, 2009.

[11] Kumar, G. and K. P. Ray, *Broadband Microstrip Antenna*, Artech House, 2003.

[12] Elsadek, H. and D. M. Nashaat, "Multiband and UWB V-shaped antenna configuration for wireless communications applications," *IEEE Antennas and Wireless Propagation Letters*, Vol. 7, 89–91, 2008.

[13] Bahl, I. J., S. S. Stuchly, and M. A. Stuchly, "A new microstrip radiator for medical applications," *IEEE Transactions on Microwave Theory and Techniques*, Vol. 28, No. 12, 1464–1469, 1980.

[14] Bahal, I. J. and P.Bartia, *Microstrip Patch Antenna*, Artech House, 1980.

[15] Tak, J., S. Woo, J. Kwon, and J. Choi, "Dual-band dual-mode patch antenna for on-/off-body WBAN communications," *IEEE Antennas and Wireless Propagation Letters*, Vol. 15, 348–351, 2015.

[16] Chung, K. L. and C.-H. Wong, "Wang-shaped patch antenna for wireless communications," *IEEE Antennas and Wireless Propagation Letters*, Vol. 9, 638–640, 2010.

[17] Gosalia, K. and G. Lazzi, "Reduced size, dual-polarized microstrip patch antenna for wireless communications," *IEEE Transactions on Antennas and Propagation*, Vol. 51, No. 9, 2182–2186, 2003.

[18] Jofre, L., M. S. Hawley, A. Broquetas, E. d. L. Reyes, M. Ferrando, and A. R. Elias-Fuste, "Medical imaging with a microwave tomographic scanner," *IEEE Transactions on Biomedical Engineering*, Vol. 37, No. 3, 303–312, 1990.

[19] Li, P. K., Z. H. Shao, Q. Wang, and Y. J. Cheng, "Frequency- and pattern-reconfigurable antenna for multistandard wireless applications," *IEEE Antennas and Wireless Propagation Letters*, Vol. 14, 333–336, 2014.

[20] Bakariya, P. S., S. Dwari, M. Sarkar, and M. K. Mandal, "Proximity-coupled multiband microstrip antenna for wireless applications," *IEEE Antennas and Wireless Propagation Letters*, Vol. 14, 646–649, 2014.

[21] Nilavalan, R., I. J. Craddock, A. Preece, J. Leendertz, and R. Benjamin, "Wideband microstrip patch antenna design for breast cancer tumour detection," *IET Microwaves, Antennas & Propagation*, Vol. 1, No. 2, 277–281, 2007.

[22] Rao, S., A. Singh, A. K. Bhat, Durgaprasad, and K. Shet, "Reactively loaded stripline fed rectangular patch antenna for wireless and biomedical applications," *Progress In Electromagnetics Research C*, Vol. 128, 219–229, 2023.

[23] Rao, S., A. Singh, A. K. Bhat, and R. Shetty, "Tumor detection using microstrip patch antenna operating in FCC MBAN band," *Progress In Electromagnetics Research C*, Vol. 136, 215–227, 2023.

[24] Terman, F. E., *Electronic and Radio Engineer*, Kagakasha, 1995.

[25] Cheng, X., D. E. Senior, C. Kim, and Y.-K. Yoon, "A compact omnidirectional self-packaged patch antenna with complementary split-ring resonator loading for wireless endoscope applications," *IEEE Antennas and Wireless Propagation Letters*, Vol. 10, 1532–1535, 2011.

[26] Liang, Z., J. Liu, Y. Li, and Y. Long, "A dual-frequency broadband design of coupled-fed stacked microstrip monopolar patch antenna for WLAN applications," *IEEE Antennas and Wireless Propagation Letters*, Vol. 15, 1289–1292, 2015.

[27] Alshehri, S. A., S. Khatun, A. B. Jantan, R. Abdullah, R. Mahmood, and Z. Awang, "Experimental study of breast cancer detection using UWB imaging," in *Proceeding of the International Conference on Advanced Science, Engineering and Information Technology*, Selangor, Malaysia, Jan. 2011.